

Article

Investigation of Ion Release and Antibacterial Properties of TiN-Cu-Nanocoated Nitinol Archwires

Bojana Ilić ^{1,*}, Božana Petrović ¹, Jelena Marinković ¹, Jadranka Miletić Vukajlović ¹, Momir Stevanović ², Jelena Potočnik ¹ and Vukoman Jokanović ^{1,3}

¹ Vinca Institute of Nuclear Sciences, National Institute of the Republic of Serbia, University of Belgrade, 11351 Belgrade, Serbia; bozana@vin.bg.ac.rs (B.P.); vukoman@vin.bg.ac.rs (V.J.)

² Faculty of Medical Sciences, University of Kragujevac, 34000 Kragujevac, Serbia

³ Albos doo, Orahovačka 19, 11000 Belgrade, Serbia

* Correspondence: bcetenovic@vin.bg.ac.rs

Abstract: Background: The use of nitinol (NiTi) archwires in orthodontic treatment has increased significantly due to unique mechanical properties. The greatest obstacle for safe orthodontic treatment is chemically or microbiologically induced corrosion, resulting in nickel (Ni) release. The aim of this investigation was to enhance corrosion resistance and introduce antibacterial properties to NiTi archwires by coating them with copper (Cu) doped titanium nitride (TiN-Cu). Methods: NiTi archwires were coated with TiN-Cu using cathodic arc evaporation (CAE) and direct current magnetron sputtering (DC-MS). The morphology of the sample was analyzed via field emission scanning electron microscopy (FESEM) and chemical composition was assessed using energy-dispersive X-ray spectroscopy (EDS), X-ray diffraction (XRD) and Fourier transformed infrared spectroscopy (FTIR). Inductively coupled plasma optical emission spectrometry (ICP-OES) was used to estimate the ion release. The biocompatibility of samples was investigated using 3-(4,5-dimethylthiazol-2-yl)-2,5-diphenyl tetrazolium bromide (MTT) assay. Antibacterial activity was tested against *Streptococcus mutans* and *Streptococcus mitis*. Results: Physicochemical characterization revealed well-designed coatings with the presence of TiN phase with incorporated Cu. TiN-Cu-nanocoated archwires showed a statistically lower Ni release ($p < 0.05$). Relative cell viability was the highest in 28-day eluates of TiN-Cu-nanocoated archwires ($p < 0.05$). The most remarkable decrease in *Streptococcus mitis* concentrations was observed in the case of TiN-Cu-coated archwires ($p < 0.05$). Conclusion: Taking into account biocompatibility and antibacterial tests, TiN-Cu-nanocoated archwires may be considered as a good candidate for further clinical investigations.

Keywords: antibacterial activity; orthodontic archwires; *Streptococcus mutans*; nanocoatings



Citation: Ilić, B.; Petrović, B.; Marinković, J.; Miletić Vukajlović, J.; Stevanović, M.; Potočnik, J.; Jokanović, V. Investigation of Ion Release and Antibacterial Properties of TiN-Cu-Nanocoated Nitinol Archwires. *Coatings* **2023**, *13*, 1587. <https://doi.org/10.3390/coatings13091587>

Academic Editor: Ajay Vikram Singh

Received: 11 August 2023

Revised: 5 September 2023

Accepted: 6 September 2023

Published: 12 September 2023



Copyright: © 2023 by the authors. Licensee MDPI, Basel, Switzerland. This article is an open access article distributed under the terms and conditions of the Creative Commons Attribution (CC BY) license (<https://creativecommons.org/licenses/by/4.0/>).

1. Introduction

The high prevalence of malocclusion in children is a consequence of genetic predisposition, bad habits, or the early loss of deciduous teeth as a result of dental caries, dental trauma, muscle dysfunctions or medications taken on daily bases [1]. The aim of orthodontic treatment (OT) is to accomplish and maintain an optimal occlusal relationship necessary to provide satisfactory oral function and aesthetic appearance.

During the 1960s, a new alloy made of nickel (Ni) and titanium (Ti) named nitinol (NiTi) was developed by W. F. Buehler at the Naval Ordnance Laboratory. The use of NiTi archwires in orthodontic applications has expanded significantly due to unique mechanical properties such as shape memory effect and superelasticity [2]. Despite these favorable properties, the greatest barrier to safe OT is the chemically or microbiologically induced corrosion of NiTi archwires. When placed in the oral environment, NiTi archwires are exposed to temperature and pH changes as a result of food, drinks, and oral health product abrasions, which all lead to surface degradation and corrosion [3,4]. The corrosion of NiTi archwires results in Ni ion release, which acts on the local and systemic level, resulting

in various health implications [5]. The synergy of different bacterial strains can affect the corrosion process directly (reduction and oxidation) or indirectly by creating metabolites that reduce the pH value of saliva. Locally, released Ni ions induce gingival overgrowth and inflammation [6], significantly compromising the OT and leading to periodontitis. It also increases bacterial adhesion and biofilm formation [7], which provokes the demineralization of the enamel and the formation of white spot lesions (WSL) [8]. Additionally, a significant increase in micronuclei in the buccal epithelial cells in children suggest its high genotoxicity and carcinogenicity [9,10].

Systemic effects of Ni exposure should not be neglected either, since Ni is known as a strong immunologic sensitizer among 28.5% of the population, especially among children and adolescents [11,12]. Hypersensitivity, allergic contact dermatitis, and metal toxicity that increases the urinary excretion of Ni, leading to renal tubular dysfunction, are the most common adverse effects attributed to its exposure [9,13].

Considering health consequences, the necessity for developing novel material coating that would preserve the mechanical properties of NiTi archwires but decrease or eliminate Ni ion release and improve biological properties is of great importance. A highly satisfactory solution for the NiTi surface modification may be the use of TiN as a very hard coating that is well-adjusted to high mechanical loads and prevents the leaching of metal ions [14,15]. It was reported that TiN coating reduced the corrosion rate of NiTi by 50% and Ni leaching by 35% in simulated blood [16].

To obtain optimal coatings for orthodontic archwires, besides corrosion resistance and the prevention of ion leaching, the introduction of antibacterial properties would be precious. In order to introduce antibacterial properties to NiTi archwires, most commonly used inorganic nanoparticles are silver (Ag) and titanium dioxide (TiO_2) [17]. Arising issues of nano-Ag safety and increased friction with respect to TiO_2 nanocoatings [18] mean that different strategies must be implemented. Copper (Cu) nanoparticles possess antibacterial effects against different bacterial strains [19]. Moreover, Cu is one of the essential elements in cell metabolism, cell proliferation, and differentiation, as well as in the fight against cancer [20]. It is estimated that the maximum Cu content of 2% wt in coatings is biocompatible, making it suitable for the NiTi archwire surface modification [21].

Different methods of physical and chemical deposition processes have been used in order to modify the surface of NiTi archwires thus far [18,22]. Despite the many advantages, the precursors to chemical deposition processes are toxic and unstable at room temperature. On the other hand, the shape and size of the coatings may be controlled when using physical deposition processes [18]. We hypothesize that by applying combined technologies of cathodic arc evaporation (CAE) and direct current magnetron sputtering (DC-MS) in the deposition process of TiN nanocoatings with the incorporation of Cu, Ni release can be prevented and a higher corrosion resistance and biocompatibility can be achieved with the simultaneous introduction of antibacterial properties. Namely, the CAE method involves thermal evaporation, where material is heated in vacuum until its vapor pressure becomes greater than the ambient pressure [22], and DS-MS implicates ion sputtering, during which the high-energy ions hit a solid and integrates inside the thin layers of materials used as a target [22]. All these will obtain stable coatings and ensure the safe usage of NiTi archwires during OT.

Based on the introductory information, the aim of this study was to coat NiTi archwires with TiN-Cu by applying combined technologies of CAE and DC-MS and further investigate ion release and antibacterial properties in comparison to NiTi and stainless steel (SS) archwires.

2. Materials and Methods

2.1. Deposition of the Films

The TiN-Cu coatings were deposited on the surface of NiTi archwires (substrate, Superelastic NiTi, OC Orthodontics, McMinnville, OR, USA, 0.018 × 0.025 inch) via the reactive CAE and DC-MS. The magnetron source for Cu sputtering was installed on one

side of the vacuum chamber, while the circular titanium cathode for the arc evaporation was placed on the opposite side.

Prior to deposition, the substrate was ultrasonically cleaned in trichlorethylene, rinsed with alcohol, and then dried with nitrogen (N) gas. Argon (Ar) (0.4 Pa, 5 min) was used for chamber cleaning while substrate bias was -700 V. During a period of 5 min, Ti interlayer was deposited on the substrate surface in the Ar atmosphere ($p = 0.4$ Pa) and with substrate bias of -200 V. Then, during a period of 10 min, TiN interlayer was deposited using N ($p = 0.4$ Pa) and a substrate bias of -200 V. In order to deposit TiN-Cu coatings, the DC-MS of Cu and the CAE of Ti were simultaneously used in N atmosphere. During a deposition period of 30 min, substrate bias was -150 V, Cu power density was $0\text{--}5.2$ W/cm 2 , substrate temperature was 250 °C, rotation speed was 16 rpm, and the distance (target–substrate) was 150 mm.

2.2. Physicochemical Characterization of the Films

Field emission scanning electron microscopy with an energy dispersive X-ray spectrometer (FESEM-EDS, FEI SCIOS 2, Dual beam, Field Electron and Ion Company, Hillsboro, OR, USA) was used to analyze the sample's morphology and composition. The micrographs were captured at an acceleration voltage of 6 kV. On the other hand, EDS measurement was performed at a voltage of 10 kV and 50 kx magnification. The sample was placed on a sample holder using double-sided adhesive carbon tape, after being sputter-coated with gold (Au) in order to increase conductivity.

Structural analysis of the coated NiTi wire was performed via X-ray diffraction (XRD) and Fourier transformed infrared spectroscopy (FTIR). XRD analysis was performed using Philips PW 1050 diffractometer with Cu-K α 1-2 lamp by collecting the data in the 2θ range from 15 to 80°, in steps of 0.055° and an exposure time of 2 s per step. In order to implement FTIR analysis, the spectrometer 380 Nicolet FTIR, Thermo Electron Corporation, was used. FTIR spectra were taken in the spectral range from 4000 to 400 cm $^{-1}$.

2.3. Inductively Coupled Plasma Optical Emission Spectroscopy

The investigated archwires (1 cm length, 0.018×0.025 inch) were placed in Petri-dishes ($n = 3$ per archwire) and immersed in 20 mL of ultrapure water ($\text{pH} = 5.76 \pm 0.51$; conductivity of 0.055 mS/cm; Barnstead GenPure Pro; Thermo Scientific, Karlsruhe, Germany) or acidic solution ($\text{pH} = 4.25 \pm 0.51$) for 7 days, 21 days, and 28 days. The concentrations of Ni, Ti, and Cu ions in solution samples were measured by inductively coupled plasma optical emission spectroscopy (ICP-OES) ($n = 3$). ICP-OES analysis was conducted via Thermo Scientific iCAP 6500 Duo ICP (Thermo Fisher Scientific, Cambridge, UK).

2.4. MTT Cytotoxicity Assay

The apical papilla of the healthy immature premolars extracted for orthodontic reasons (Ethics Committee 116-19-2/2020-000) was used for the isolation of stem cells from the apical papilla (SCAPs). Tissue fragments were washed twice in phosphate-buffered saline (PBS, Sigma-Aldrich, St. Louis, MO, USA) and transferred into tissue culture dishes with 100 μ L Dulbecco's Modified Eagle's Medium (DMEM/F12; Thermo Fisher Scientific, Inc., Valtam, Sheridan, WY, USA), enriched with 20% fetal bovine serum (FBS; Thermo Fisher Scientific, Inc.) and 1% antibiotic/antifungal (ABAM; Thermo Fisher Scientific, Inc.). After 10 days of incubation at 37 °C in a humidity of 5% CO $_2$, fragments were removed. Once monolayered confluence was obtained, cells were washed with PBS and detached using 0.25% Trypsine (Sigma-Aldrich) and re-cultured. The characterization of cells was determined using the flow cytometry (Partec, Munster, Germany) and conjugated monoclonal antibodies for membrane markers CD90 (FITC) (Life technologies, Carlsbad, CA, USA), CD73 (PB) (Sony Biotechnology, San Jose, CA, USA), CD105 (FITC) (Exbio, Prague, Czech Republic), CD34 (FITC) (Sony Biotechnology), CD45 (PE) (Exbio). In order to confirm mesenchymal potential of SCAPs, cells were cultured in different media (osteogenic/adipogenic/chondrogenic) (Miltenyi Biotec, Bergisch Gladbach, Germany).

Investigated archwires (Superelastic NiTi, OC Orthodontics, Oregon, USA—containing 55% Ni and 45% of Ti; stainless steel, American Orthodontics, Washington, DC, USA—containing 18%–20% of Cr and 8%–10% of Ni; and TiN-Cu-nanocoated archwires) were sterilized using UV lamp and then immersed in Petri dishes ($n = 6$, per archwire 0.018×0.025 -inch) containing DMEM at 37°C for 7 days, 21 days, and 28 days (w/v ratio was 0.1 mg/mL), as recommended by the International Standard Organization (ISO) 10993-5 [23]. Prior to use, the extracts were filtered to eliminate solid particles and stored at -20°C .

In order to perform 3-(4,5-dimethylthiazol-2-yl)-2,5-diphenyl tetrazolium bromide (MTT) test, cells were incubated with the culture medium (DMEM/F12) in 96-well plates. After 24 h of incubation, the culture medium was removed from well plates and 100 mL of 50% diluted and undiluted extracts were added per pool. After 24 h incubation at 37°C in an atmosphere with 5% CO_2 , 10 mL MTT solution (5 mg/mL in a phosphate buffer; Thermo Fisher Scientific, Inc.) was added per pool. After 4 h of incubation, 100 mL 10% sodium dodecylsulfate in 0.01 mol/L HCl (Serva, Heidelberg, Germany) was used per pool. The optical density (OD) was measured spectrophotometrically on enzyme-linked immunosorbent assay plate reader (Behring ELISA Processor II, Heidelberg, Germany) at a wavelength of 570 nm after 24 h ($n = 3$). The metabolic activity of cell (% M) was determined following the formula [24]:

$$\% \text{ M} = \frac{\text{OD}_{\text{cell culture with samples}} - \text{OD}_{\text{samples without cell culture}}}{\text{OD}_{\text{cell culture without samples}} - \text{OD}_{\text{control medium}}} \times 100$$

2.5. Bacterial Adhesion and Biofilm Formation

Bacterial cultivation of *Streptococcus mutans* and *Streptococcus mitis* isolates was performed by the streaking of frozen stock cultures onto Mueller–Hinton agar (MHA, Oxoid) and incubated for 72 h at 37°C . Single colonies of *Streptococcus mutans* and *Streptococcus mitis* were inoculated into Tryptone soya Broth (TSB, HiMedia, Mumbai, India) and grown overnight at 37°C . Cell suspensions were adjusted spectrophotometrically to an optical density, OD_{600} , of 0.2 (corresponding to $1 \times 10^8 \text{ CFU mL}^{-1}$).

In order to test biofilm adhesion and to quantify adherent bacteria onto investigated archwires, modified plate counting assay [25] was used as follows: under sterile conditions, 1 cm of archwire was immersed in 1 mL of the bacterial suspension ($1 \times 10^6 \text{ CFU mL}^{-1}$ in TSB enriched with 0.5% of glucose) and settled in each well of 24-well plates. After 72 h of incubation at 37°C , each archwire was removed from the well and placed into Eppendorf tubes containing 1 mL of sterile TSB. After 15 min in ultrasonic bath (Sonorex, Bandelin Electronic, Berlin, Germany) and 2 min of the vortex, both being used to disturb biofilm settled on the wire, aliquots (100 μL) of concentrated or serially diluted (10^{-1} and 10^{-5}) medium were seeded on MHA. After 48 h of incubation at 37°C , CFUs mL^{-1} were calculated. Two individual experiments in quadruplicate were performed.

2.6. Statistical Analysis

After conducting Kolmogorov–Smirnov test, statistical analysis was performed by using the repeated-measures analysis of variance (post hoc Tukey test). The level of significance was set at $p < 0.05$, and data were processed by using the statistical software IBM SPSS (IBM SPSS 20; IBM Corporation, Armonk, NY, USA).

3. Results

3.1. FESEM

Representative FESEM micrographs taken from TiN-Cu-coated archwire were recorded at low and high magnifications and are presented in Figure 1a and b, respectively. From Figure 1a, it is abundantly evident that the deposited Cu is evenly distributed over the sample, thus exhibiting uniform surface morphology. In addition, Figure 1b shows that the Cu particles grew in the form of a spherical-like or elongated (rod-like) structure, as well as their agglomerations. The analysis of the particles' sizes revealed that the diameter of spherical

particles was in the range from 20 nm to 130 nm, with the majority having an average diameter over the 50 nm. In the case of elongated Cu particles, the width was found to vary between 40 nm and 120 nm, with particle length values reaching up to 300 nm.

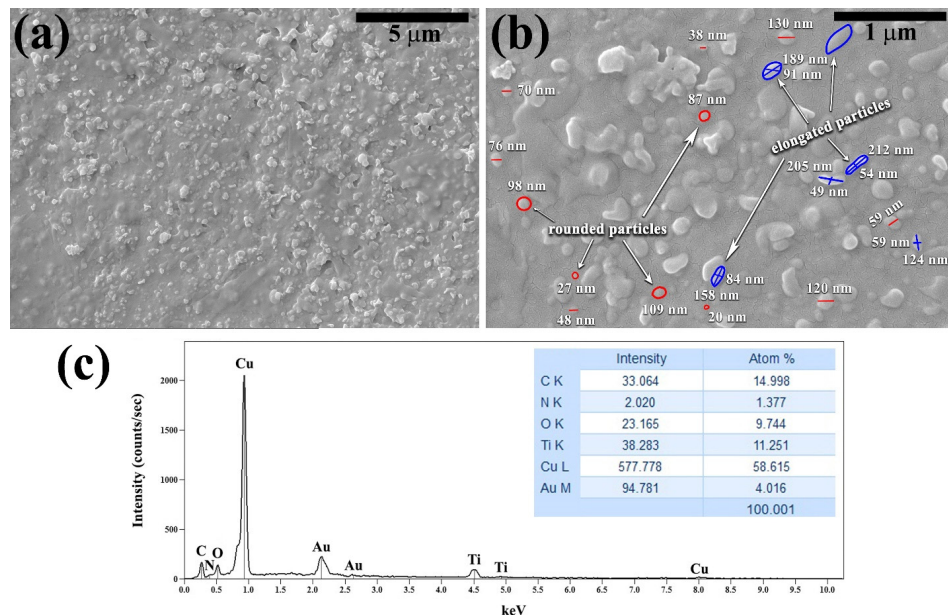


Figure 1. FESEM micrographs of the TiN-Cu-coated archwire recorded at different magnifications: (a) 5 kx and (b) 50 kx; (c) corresponding EDS spectrum (inset: maximum intensities and atomic percentages obtained for each element).

3.2. EDS

In order to verify the chemical composition of the sample, EDS analysis was also carried out, and the typical EDS spectrum is shown in Figure 1c, covering the energy range of 0.1–10 keV. The most intensive peak recorded at 0.928 keV energy belongs to Cu, whereas the smaller peaks were also observed, which were related to carbon (C), oxygen (O), N, and Ti. The presence of both N and Ti peaks confirms the existence of TiN layer. In addition, EDS spectrum also exhibits characteristic peaks that correspond to gold (Au), which are due to the sample's preparation for FESEM-EDS analysis.

3.3. XRD

XRD analysis confirmed the presence of the deposited TiN phase: planes (002) and (222) at angles 42.46 and 77.64° (Figure 2). The presence of Cu is also evident at 43.49° (plane (111)) and by a small peak at 50.59° (plane (200)), which is hardly visible on the XRD pattern due to the extremely high peak of TiN.

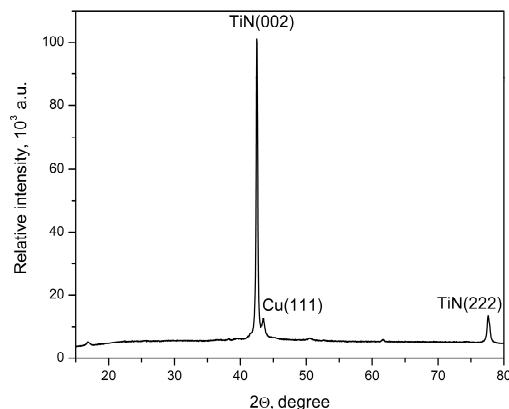


Figure 2. XRD pattern of the TiN-Cu-nanocoated archwire.

3.4. FTIR

The FTIR spectrum of the TiN-Cu-coated archwire is shown in Figure 3. The bands at 3903, 3848, and 3732 cm^{-1} can be ascribed to surface hydroxyl groups and absorbed water molecules, while bands at 3562 and 3281 cm^{-1} bands are attributed to the surface-absorbed water. The bands at 2923 and 2957 cm^{-1} can be attributed to OH radicals. The bands at 2635 and 2321 cm^{-1} can be assigned to the overtone of carbonate impurities and adsorbed CO_2 on the surface thin films, while the band at 2173 cm^{-1} can be assigned to the mode of parallel-arranged CO oscillators adsorbed on fivefold coordinated Ti^{4+} sites on the main exposed TiO_2 surfaces. This effect can be explained as the progressive vanishing of the dynamic and static lateral interactions among the CO oscillators. This frequency is associated with isolated $\text{Ti}^{4+}\dots\text{CO}$ species. This band can be assigned to CO adsorbed coordinately to unsaturated Ti^{4+} sites on (001) faces, possessing a very low electrophilicity, and on some edges. The band at 1985 cm^{-1} indicates the formation of some new species in TiO_2 during oxygen or/and nitrogen doping. The band at 1660 cm^{-1} corresponds to bending vibrations of O-H and the bands at 1555, 1511, and 1456 cm^{-1} can be assigned to the vibration of the CO_2^- inside of the carbonate impurities. The bands around 1263 cm^{-1} are described as complex vibration involving CH, COH, and CCH motions. The band at 1158 cm^{-1} corresponds to C-C (ring) stretching vibration while the band at 1103 cm^{-1} can be assigned to the asymmetric stretching vibration corresponding to the carbonyl group. The band at 1026 cm^{-1} , attributed to Ti-N stretching vibration evidences the deposition of the TiN phase. The band at 805 cm^{-1} can be assigned to the formation of multiply bonded TiO species, while the band at 546 cm^{-1} can be attributed to Ti-N stretching modes and Ti-O vibration in titanium oxides.

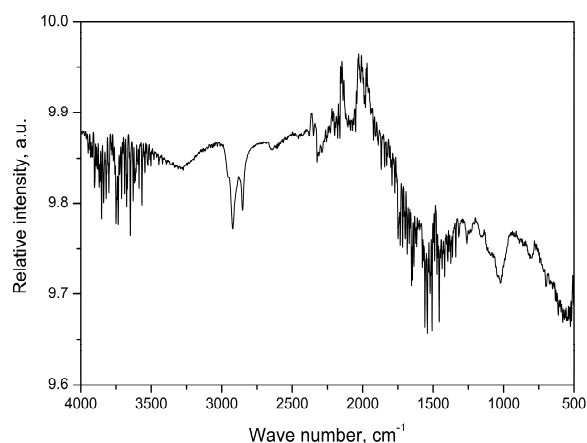


Figure 3. FTIR spectrum of the TiN-Cu-nanocoated archwire.

3.5. Ion Release Measurements

Ion releases by the investigated archwires into ultrapure water and acidic solution are presented in Table 1. Compared to NiTi and stainless steel, the TiN-Cu-nanocoated archwires showed a statistically lower release of Ni, both in ultrapure water and an acidic environment regarding all observation times ($p < 0.05$). The release of Ni increased during observation time in acidic conditions ($p < 0.05$), contrary to the neutral environment. The Ti release was the highest with regard to the NiTi archwires after 28 days in acidic conditions ($p < 0.05$). The release of Ti was constant during the experimentation period in the case of TiN-Cu-nanocoated archwires, contrary to NiTi archwires. The release of Cu was the highest regarding the TiN-Cu-nanocoated archwires after 7 days in neutral conditions ($p < 0.05$), but decreased during the experiment time, both in neutral and acidic conditions ($p < 0.05$). Chromium (Cr) was the highest in the case of SS archwires and increased during the experimentation period in an acidic environment ($p < 0.05$).

Table 1. Ion release into different solutions (ppb; mean value \pm standard deviation).

Ion	TiN-Cu-Coated Archwire			NiTi Archwire			SS Archwire		
	7 Days	21 Days	28 Days	7 Days	21 Days	28 Days	7 Days	21 Days	28 Days
Ti water	2.8 \pm 0.2	3.8 \pm 0.1	4.1 \pm 0.1	3.1 \pm 0.2	3.0 \pm 0.1	3.1 \pm 0.1	1.6 \pm 0.1	1.8 \pm 0.2	1.7 \pm 0.2
Ti acid	929 \pm 12	958 \pm 20	963 \pm 19	354 \pm 9	1144 \pm 23	1398 \pm 31	6.9 \pm 0.2	2.9 \pm 0.1	7.4 \pm 2.9
Ni water	6.1 \pm 0.1	6.1 \pm 0.1	1.7 \pm 0.1	33.9 \pm 0.1	21.0 \pm 0.1	19.7 \pm 0.2	3.5 \pm 0.1	3.7 \pm 0.3	3.7 \pm 0.2
Ni acid	59.9 \pm 0.8	1429 \pm 29	1443 \pm 21	555 \pm 5	1917 \pm 15	2129 \pm 20	49 \pm 2	75.7 \pm 3	111 \pm 2
Cu water	1210 \pm 0.8	1010 \pm 0.2	956 \pm 0.4	49.8 \pm 0.2	71.6 \pm 0.8	119 \pm 1.2	46.8 \pm 0.5	30.3 \pm 0.8	13 \pm 1.2
Cu acid	1020 \pm 1.2	961 \pm 0.4	879 \pm 0.7	59.3 \pm 0.4	78.2 \pm 0.2	128.1 \pm 0.1	82.4 \pm 0.2	40.1 \pm 0.1	25.6 \pm 1.0
Cr water	<1	<1	<1	<1	<1	<1	<1	<1	<1
Cr acid	1.7 \pm 0.2	2.0 \pm 0.3	2.1 \pm 0.1	2.5 \pm 0.4	3.4 \pm 0.1	3.8 \pm 0.2	32.6 \pm 1.5	41.8 \pm 1.2	50.4 \pm 1.8

3.6. MTT Analysis

The metabolic activity was the highest after day 28 of extraction time in the case of TiN-Cu-nanocoated archwires ($p < 0.05$), and slightly increased during this time for all investigated archwires (Figures 4 and 5). There were statistically significant differences in metabolic activity between undiluted TiN-Cu-nanocoated samples and NiTi samples after 7 and 28 days of extraction; as well as between TiN-Cu-nanocoated samples and SS samples for all of the observation period ($p < 0.05$). Statistically significant differences between diluted eluates were observed at all of the observation periods ($p < 0.05$).

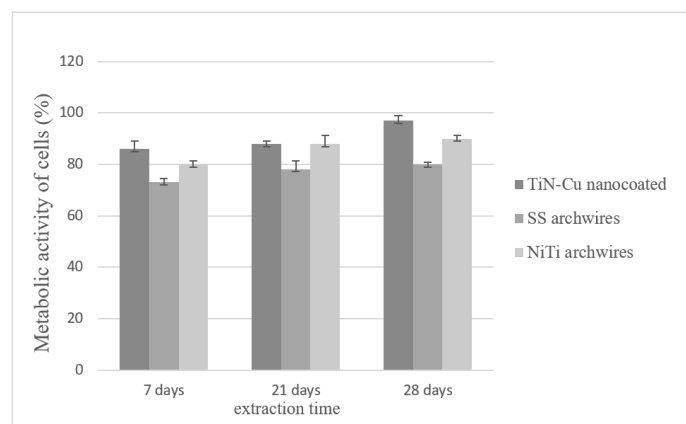


Figure 4. Metabolic activity of cells (%) after exposure to undiluted (100%) eluates of investigated archwires.

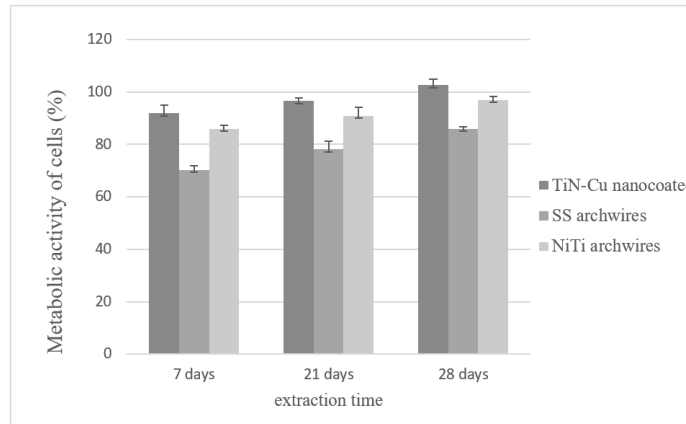


Figure 5. Metabolic activity of cells (%) after exposure to diluted (50%) eluates of investigated archwires.

3.7. Antibacterial Analysis

The final bacterial count for *Streptococcus mutans* and *Streptococcus mitis* regarding all of the investigated archwires are presented in Table 2. The inhibitor effect of TiN-Cu-nanocoated NiTi archwires was observed against *Streptococcus mutans* and *Streptococcus mitis* ($p < 0.05$, Table 2). The lowest decrease in bacterial count was noticed for the SS archwires. The most remarkable decrease in *Streptococcus mitis* concentrations was observed in the case of TiN-Cu-nanocoated archwires ($p < 0.05$). Although the control groups demonstrated decreases in bacterial count, the TiN-Cu-nanocoated archwires showed the most drastic decreases ($p < 0.05$).

Table 2. Final bacterial count for *Streptococcus mutans* and *Streptococcus mitis*.

	<i>Streptococcus mutans</i>			<i>Streptococcus mitis</i>		
	TiN-Cu-Nanocoated Archwires	NiTi Archwires	SS Archwires	TiN-Cu-Nanocoated Archwires	NiTi Archwires	SS Archwires
Log CFU \pm SD	4.19 \pm 0.22	4.29 \pm 0.24	5.87 \pm 1.10	3.08 \pm 0.99	3.75 \pm 0.82	5.54 \pm 0.60

4. Discussion

The coating of NiTi archwires in this study was performed by the simultaneous application of two methods of physical vapor deposition: the CAE and DC-MS methods. As a method, CAE is predominantly used for the deposition of high-density nitride and some oxide coatings with improved adhesion [22]. DC-MS shows numerous advantages over other methods of physical vapor deposition due to its high rate and diverse metal/alloys coatings' deposition on the surface of various materials with improved adhesion and excellent coverage [22]. By applying the described technologies, we intended to modify the surface of NiTi archwires with multilayer coatings of high hardness, abrasion resistance, and fine nanostructures, while also providing the long-term chemical, thermal, and environmental stability, which is essential for safe clinical use.

The FESEM characterization of the designed coatings showed that the Cu nanoparticles (20 nm to 130 nm) were evenly distributed on the TiN surface, with well organized spherical and elongated particles as well as their agglomerations. Such topography promotes corrosion resistance and consequently increases biocompatibility, due to decreased surface roughness [18]. In addition, favorable mechanical properties, especially a lower friction, may be achieved, which is very crucial during OT [18]. Furthermore, EDS spectrum confirmed the existence of Cu, Ti, and N in the samples, while XRD and FTIR analyses showed the presence of the TiN phase with incorporated Cu, which indicated that the desired phases were obtained.

Bearing in mind the hypersensitivity to Ni, especially in the female population, and although the released concentrations were lower than permitted [26], the potential systemic effect or synergistic effects with other metal ions must not be neglected. Ni ion release was lower in the case of TiN-Cu-nanocoated archwires in both acidic and neutral environments. This result indicates that synthesized nanocoatings reduce Ni ion release comparably to other results [27,28]. It is well known that Ti is biocompatible primarily due to the spontaneous formation of passivation layers, but an increase in Ti release may be an indicator of surface degradation and corrosion [29]. Although Ti is not considered as a metal that causes allergic reactions, there are studies showing that it can cause type IV or type I hypersensitivity reactions in patients with dental implants [30]. In our study, the release of Ti in an acidic medium was constant during the observation period, comparably to other findings [27,31]. Also, its cumulative release was lower compared to NiTi archwires, leading to the conclusion that TiN-Cu nanocoatings increased the corrosion resistance of NiTi archwires, which is crucial when biocompatibility is of great concern. As expected, the release of Cu was the highest, regarding the TiN-Cu-nanocoated archwires. Interestingly, the release of Cu was lower in acidic conditions compared to neutral, but remained below the maximum allowed levels [32]. In the present study, all investigated archwires exhibited

favorable biocompatibility. The obtained results suggest that applied technologies provided well-designed nanocoatings with the ion release rate not influencing their biocompatibility and cell viability. These findings are comparable to previous results that revealed no cytotoxic effect of the NiTi archwires [33,34]. The release of Cr increased with time in an acidic environment, comparable to the study of Laird et al. [35]. Furthermore, the lowest metabolic activity observed in the case of SS archwires may be attributed to the highest Cr ion release. Besides NiTi archwires, the most commonly used type during OT are SS archwires. Therefore, it was the main reason we have included SS archwires in the present study.

When introducing antibacterial properties to NiTi archwires, the first strategy may be to create an antiadhesive surface that is protected from biofilm formation. The second is to design coatings while incorporating antibacterial substances that can also be released [19]. The antibacterial mechanism of metallic nanoparticles is based on their reaction with oxygen, producing different types of reactive oxygen species (ROS). Leached metal ions may directly interact with bacterial cell walls or through electrostatic interactions (positively charged ions interact with the negatively charged membrane lipoproteins), resulting in bacterial death. Furthermore, once metal nanoparticles enter a bacterial cell, they may cause impairing damage to the DNA or disturb bacterial metabolism [19]. Different inorganic metals with antibacterial effects have been used for the introduction of antibacterial properties to NiTi archwires thus far [19]. To the best of our knowledge, no previous studies investigated the antibacterial properties of nano-Cu incorporated into archwire coatings. Cu is involved in vital cellular functions, taking part in metabolic processes and enzyme activities [20]. The exact mechanism by which Cu achieves its antibacterial potential has not been precisely determined, but it is believed that the synergism of all the described models plays a role [20].

The prevalence of WSL in the first six months of the fixed OT is 38% and 50% at the end of the treatment [8]. Therefore, by applying antibacterial coatings, the overall complications requiring professional care and an annual cost will be reduced [36]. In order to assess the antibacterial activity of TiN-Cu nanocoatings, we have investigated the adhesion of the *Streptococcus mutans* and *Streptococcus mitis* colonies to the wires. *Streptococcus mitis* is considered as primary colonizers of the dental biofilm, forming over 80% of the initial biofilm with other *Streptococci* [37]. *Streptococcus mutans* is one of the main causative of WSL, enabling the adhesion of other cariogenic bacteria by producing glucans while catalyzing sucrose [37]. Antibacterial tests indicated a significant decrease in *Streptococcus mutans* and *Streptococcus mitis* counts, regarding TiN-Cu-nanocoated archwires. In contrast, TiN coatings showed no reduction in *Streptococcus mutans* [38,39], indicating the importance of copper in the obtained results.

Recent studies showed that the antibacterial effects of nano-Cu not only depend on size, but also on particles' morphology and bacterial strain nature [40,41]. Different results acquired with regard to the nano-Cu particle size may be attributed to the usage of different bacterial strains and methodologies applied. Spherical-shaped Cu nanoparticles showed more antibacterial properties on Gram-positive bacteria than on Gram-negative bacteria [40,41]. These findings support our result because both investigated bacterial strains are Gram-positive.

5. Conclusions

In the current investigation, TiN-Cu nanocoatings obtained using the combined technologies of cathodic arc evaporation and DC magnetron sputtering were evaluated in terms of biocompatibility, ion release, and antibacterial properties. It was shown that the designed TiN-Cu nanocoatings on the surface of the NiTi archwires were stable, both in neutral and acidic environments. Biocompatibility tests on cell lines showed the safety of the investigated TiN-Cu-nanocoated archwires. The amount of Ni ion release from the investigated TiN-Cu-nanocoated archwires were within the safety limit and were significantly lower when compared to uncoated NiTi archwires. Antibacterial tests indicated a decrease in

Streptococcus mutans and *Streptococcus mitis* counts; so, TiN-Cu-nanocoated archwires may be considered as a good candidate for further clinical investigations.

Author Contributions: Conceptualization, B.I., B.P. and V.J.; Formal analysis, J.M.V.; Investigation, B.I., B.P., J.M., J.M.V., M.S. and J.P.; Writing—original draft, B.I. and B.P.; Writing—review & editing, J.M., M.S., J.P. and V.J.; Supervision, V.J. All authors have read and agreed to the published version of the manuscript.

Funding: This research was funded by the Ministry of Science, Technological Development and Innovation of the Republic of Serbia (Contract No. 451-03-47/2023-01/200017).

Institutional Review Board Statement: The study was conducted in accordance with the Declaration of Helsinki, and approved by the Ethics Committee of Vinca Institute of Nuclear Sciences, National Institute of the Republic of Serbia, University of Belgrade, Serbia (protocol code 116-19-2/2020-000 and 18 September 2020).

Informed Consent Statement: Informed consent was obtained from all subjects involved in the study.

Data Availability Statement: Data sharing is not applicable to this article.

Conflicts of Interest: The authors declare no conflict of interest.

References

1. American Dental Association (ADA). Oral Health and Well-Being in the United States. Available online: <https://www.ada.org/resources/research/health-policy-institute/coverage-access-outcomes/oral-health-and-well-being> (accessed on 9 June 2023).
2. Nespoli, A.; Passaretti, F.; Szentmiklósi, L.; Maróti, B.; Placidi, E.; Cassetta, M.; Yada, R.Y.; Farrar, D.H.; Tian, K.V. Biomedical NiTi and β -Ti Alloys: From Composition, Microstructure and Thermo-Mechanics to Application. *Metals* **2022**, *12*, 406. [[CrossRef](#)]
3. Papadopoulou, K.; Eliades, T. Microbiologically-influenced corrosion of orthodontic alloys: A review of proposed mechanisms and effects. *Aust. Orthod. J.* **2009**, *25*, 63–75. [[PubMed](#)]
4. Rincic Mlinaric, M.; Karlovic, S.; Ciganj, Z.; Pop Acev, D.; Pavlic, A.; Spalj, S. Oral antiseptics and nickel titanium alloys: Mechanical and chemical effect of interaction. *Odontology* **2019**, *107*, 150–157. [[CrossRef](#)] [[PubMed](#)]
5. Kulkarni, P.; Agrawal, S.; Bansal, A.; Jain, A.; Tiwari, U.; Anand, A. Assessment of nickel release from various dental appliances used routinely in pediatric dentistry. *Indian J. Dent.* **2016**, *7*, 81–85. [[CrossRef](#)]
6. Gursoy, U.K.; Sokucu, O.; Utto, V.J.; Aydin, A.; Demirer, S.; Toker, H.; Erdem, O.; Sayalet, A. The role of nickel accumulation and epithelial cell proliferation in orthodontic treatment-induced gingival overgrowth. *Eur. J. Orthod.* **2007**, *29*, 555–558. [[CrossRef](#)]
7. Amauri, J.P.; Hwang, G.; Koo, H. Dynamics of bacterial population growth in biofilms resemble spatial and structural aspects of urbanization. *Nat. Commun.* **2020**, *11*, 1354.
8. Lucchese, A.; Gherlone, E. Prevalence of white-spot lesions before and during orthodontic treatment with fixed appliances. *Eur. J. Orthod.* **2012**, *35*, 664–668. [[CrossRef](#)]
9. Morán-Martínez, J.; Monreal-de Luna, K.D.; Betancourt-Martínez, N.D.; Carranza-Rosales, P.; Contreras-Martínez, J.G.; López-Meza, M.C.; Rodríguez-Villarreal, O. Genotoxicity in oral epithelial cells in children caused by nickel in metal crowns. *Genet. Mol. Res.* **2013**, *12*, 3178–3185. [[CrossRef](#)]
10. Alp, G.; Çakmak, G.; Sert, M.; Burgaz, Y. Corrosion potential in artificial saliva and possible genotoxic and cytotoxic damage in buccal epithelial cells of patients who underwent Ni-Cr based porcelain-fused-to-metal fixed dental prostheses. *Mutat. Res./Genet. Toxicol. Environ. Mutagen.* **2018**, *827*, 19–26.
11. Sfondrini, M.F.; Cacciafiesta, V.; Maffia, E.; Scribante, A.; Alberti, G.; Biesuz, R.; Klersy, C. Nickel release from new conventional stainless steel, recycled, and nickel free orthodontic brackets: A *in vitro* study. *Am. J. Orthod. Dentofac. Orthop.* **2009**, *137*, 809–815. [[CrossRef](#)]
12. Biesiekierski, A.; Wang, J.; Gepreel, M.A.; Wen, C. A newlook at biomedical Ti-based shape memory alloy. *Acta Biomater.* **2012**, *8*, 1661–1669.
13. Das, K.K.; Reddy, R.; Bagoji, I.B.; Das, S.; Bagali, S.; Mullur, L.; Khodnapur, J.P.; Biradar, M.S. Primary concept of nickel toxicity—An overview. *J. Basic Clin. Physiol. Pharmacol.* **2018**, *30*, 141–152.
14. Ikeda, D.; Ogawa, M.; Hara, Y.; Nishimura, Y.; Odusanya, O.; Azuma, K.; Satoshi Matsuda, S.; Yatsuzuka, M.; Murakami, A. Effect of nitrogen plasma-based ion implantation on joint prosthetic material. *Surf. Coat. Technol.* **2002**, *156*, 301–305.
15. Weng, K.; Chen, Y.; Lin, T.; Wang, D. Characterization of Titanium Nitride Coatings Deposited by Metal Plasma Ion Pre-Implantation and Cathodic Arc Evaporation. *J. Nanosci. Nanotechnol.* **2009**, *9*, 1127–1132. [[CrossRef](#)] [[PubMed](#)]
16. Gill, P.; Musaramthota, V.; Munroe, N.; Datye, A.; Dua, R.; Haider, W.; McGoron, A.; Rokicki, R. Surface modification of Ni-Ti alloys for stent application after magnetoelectropolishing. *Mater. Sci. Eng. C Mater. Biol. Appl.* **2015**, *50*, 37–44. [[PubMed](#)]
17. Wang, N.; Yu, J.; Yan, J.; Hua, F. Recent advances in antibacterial coatings for orthodontic appliances. *Front. Bioeng. Biotechnol.* **2023**, *11*, 1093926. [[PubMed](#)]

18. Bącela, J.; Łabowska, M.B.; Detyna, J.; Zięty, A.; Michalak, I. Functional Coatings for Orthodontic Archwires—A Review. *Materials* **2020**, *13*, 3257. [CrossRef]
19. Godoy-Gallardo, M.; Eckhard, U.; Delgado, L.M.; de Roo Puente, Y.J.D.; Hoyos-Nogués, M.; Gil, F.J.; Perez, R.A. Antibacterial approaches in tissue engineering using metal ions and nanoparticles: From mechanisms to applications. *Bioact. Mater.* **2021**, *6*, 4470–4490.
20. Ruiz, L.M.; Libedinsky, A.; Elorza, A.A. Role of Copper on Mitochondrial Function and Metabolism. *Front. Mol. Biosci.* **2021**, *8*, 711227.
21. Chen, Z.; Meng, H.; Xing, G.; Chen, C.; Zhao, Y.; Jia, G.; Wang, T.; Yuan, H.; Ye, C.; Zhao, F.; et al. Acute toxicological effects of copper nanoparticles in vivo. *Toxicol. Lett.* **2006**, *163*, 109–120. [CrossRef] [PubMed]
22. Tudose, I.V.; Comanescu, F.; Pascariu, P.; Bucur, S.; Rusen, L.; Iacomi, F.; Koudoumas, E.; Suchea, M. Chapter 2—Chemical and physical methods for multifunctional nanostructured interface fabrication. In *Micro and Nano Technologies, Functional Nanostructured Interfaces for Environmental and Biomedical Applications*; Dinca, V., Suchea, M.P., Eds.; Elsevier: Amsterdam, The Netherlands, 2019; pp. 15–26.
23. ISO 10993-5:2009; Biological Evaluation of Medical Devices—Part 5: Tests for In Vitro Cytotoxicity. ISO: Geneva, Switzerland, 2009.
24. Cetenovic, B.; Prokic, B.; Vasilijic, S.; Dojcinovic, B.; Magic, M.; Jokanovic, V.; Markovic, D. Biocompatibility investigation of new endodontic materials based on nanosynthesized calcium silicates combined with different radiopacifiers. *J. Endod.* **2017**, *43*, 425–432. [PubMed]
25. Özyildiz, F.; Uzel, A.; Hazar, A.S.; Güden, M.; Olmez, S.; Aras, I.; Karaboz, I. Photocatalytic antimicrobial effect of TiO₂ anatase thin-film-coated orthodontic arch wires on 3 oral pathogens. *Turk. J. Biol.* **2014**, *38*, 289–295. [CrossRef]
26. Nickel—Registration Dossier—ECHA. Available online: <https://european-union.europa.eu/select-language?destination=/node/1> (accessed on 9 June 2023).
27. Sugisawa, H.; Kitaura, H.; Ueda, K.; Kimura, K.; Ishida, M.; Ochi, Y.; Kishikawa, A.; Ogawa, S.; Takano-Yamamoto, T. Corrosion resistance and mechanical properties of titanium nitride plating on orthodontic wires. *Dent. Mater. J.* **2018**, *37*, 286–292. [CrossRef]
28. Ito, A.; Kitaura, H.; Sugisawa, H.; Noguchi, T.; Ohori, F.; Mizoguchi, I. Titanium nitride plating reduces nickel ion release from orthodontic wire. *Appl. Sci.* **2021**, *11*, 9745. [CrossRef]
29. Bocchetta, P.; Chen, L.Y.; Tardelli, J.D.C.; Reis, A.C.D.; Almeraya-Calderón, F.; Leo, P. Passive Layers and Corrosion Resistance of Biomedical Ti-6Al-4V and β-Ti Alloys. *Coatings* **2021**, *11*, 487. [CrossRef]
30. Hosoki, M.; Nishigawa, K.; Miyamoto, Y.; Ohe, G.; Matsuka, Y. Allergic contact dermatitis caused by titanium screws and dental implants. *J. Prosthodont. Res.* **2016**, *60*, 213–219. [PubMed]
31. Azizi, A.; Jamilian, A.; Nucci, F.; Kamali, Z.; Hosseiniakhoo, N.; Perillo, L. Release of metal ions from round and rectangular NiTi wires. *Prog. Orthod.* **2016**, *17*, 10. [PubMed]
32. Taylor, A.A.; Tsuji, J.S.; Garry, M.R.; McArdle, M.E.; Goodfellow, W.L., Jr.; Adams, W.J.; Menzie, C.A. Critical Review of Exposure and Effects: Implications for Setting Regulatory Health Criteria for Ingested Copper. *Environ. Manag.* **2020**, *65*, 131–159.
33. Jenko, M.; Godec, M.; Kocjan, A.; Rudolf, R.; Dolinar, D.; Ovsenik, M.; Gorencsek, M.; Zaplotnik, R.; Mozetic, M. A new route to biocompatible Nitinol based on a rapid treatment with H₂/O₂ gaseous plasma. *Appl. Surf. Sci.* **2019**, *473*, 976–984.
34. Rongo, R.; Valletta, R.; Bucci, R.; Rivieccio, V.; Galeotti, A.; Michelotti, A.; D'Antò, V. In vitro biocompatibility of nickel-titanium esthetic orthodontic archwires. *Angle Orthod.* **2016**, *86*, 789–795.
35. Laird, C.; Xu, X.; Yu, Q.; Armbruster, P.; Ballard, R. Nickel and chromium ion release from coated and uncoated orthodontic archwires under different pH levels and exposure times. *J. Oral Biosci.* **2021**, *63*, 450–454. [CrossRef] [PubMed]
36. Ren, Y.; Jongsma, M.A.; Mei, L.; Van Der Mei, H.C.; Busscher, H.J. Orthodontic treatment with fixed appliances and biofilm formation—A potential public health threat? *Clin. Oral. Investig.* **2014**, *18*, 1711–1718. [PubMed]
37. Kolenbrander, P.E. Oral microbial communities: Biofilms, interactions, and genetic systems. *Annu. Rev. Microbiol.* **2000**, *51*, 413–437.
38. Teixeira, L.P.; Gontijo, L.C.; Franco Junior, A.R.; Pereira, M.F.; Schuenck, R.P.; Malacarne-Zanon, J. Evaluation of antimicrobial potential and surface morphology in thin films of titanium nitride and calcium phosphate on orthodontic brackets. *Am. J. Orthod. Dentofac. Orthop.* **2021**, *160*, 209–214.
39. Jabbari, Y.S.A.; Fehrman, J.; Barnes, A.C.; Zapf, A.M.; Zinelis, S.; Berzins, D.W. Titanium nitride and nitrogen ion implanted coated dental materials. *Coatings* **2012**, *2*, 160–178. [CrossRef]
40. Laha, D.; Pramanik, A.; Laskar, A.; Jana, M.; Pramanik, P.; Karmakar, P. Shape-dependent bactericidal activity of copper oxide nanoparticle mediated by DNA and membrane damage. *Mater. Res. Bull.* **2014**, *59*, 185–191. [CrossRef]
41. Majumdar, T.D.; Singh, M.; Thapa, M.; Dutta, M.; Mukherjee, A.; Ghosh, C.K. Size-dependent antibacterial activity of copper nanoparticles against *Xanthomonas oryzae* pv. *Oryzae*—A synthetic and mechanistic approach. *Colloid Interface Sci. Commun.* **2019**, *32*, 100190. [CrossRef]

Disclaimer/Publisher's Note: The statements, opinions and data contained in all publications are solely those of the individual author(s) and contributor(s) and not of MDPI and/or the editor(s). MDPI and/or the editor(s) disclaim responsibility for any injury to people or property resulting from any ideas, methods, instructions or products referred to in the content.